IEEE *Access*
Multidisciplinary : Rapid Review : Open Access Journal

Gesture Recognition with Ultrasounds and Edge Computing

BORJA SAEZ[1], JAVIER MENDEZ[1], MIGUEL MOLINA[1], ENCARNACION CASTILLO[2], MANUEL PEGALAJAR[3], AND DIEGO P. MORALES, .[2]

[1]Infineon Technologies AG, Am Campeon 1-15, 85579 Neubiberg, Germany
[2]Department of Electronics and Computer Technology, University of Granada, 18071 Granada, Spain
[3]Department of Computer Science and Artificial Intelligence, University of Granada, 18071 Granada, Spain

Corresponding author: Borja Saez (e-mail: Borja.SaezMingorance@infineon.com).

ABSTRACT The aim of this work is to prove that it is possible to develop a system able to detect gestures based only on ultrasonic signals and Edge devices. A set of 7 gestures plus idle has been defined, being possible to combine them to increase the recognized gestures. In order to recognize them, Ultrasound transceivers will be used to detect the 2 dimensional gestures. The Edge device approach implies that the whole data is processed in the device at the network edge rather than depending on external devices or services such as Cloud Computing. The system presented in this paper has been proven to be able to measure Time of Flight (ToF) signals that can be used to recognize multiple gestures by the integration of two transceivers, with an accuracy between 84.18% and 98.4%. Due to the optimization of the preprocessing correlation technique to extract the ToF from the echo signals and our specific firmware design to enable the parallelization of concurrent processes, the system can be implemented as an Edge Device.

INDEX TERMS Edge computing, Gesture recognition, Human System Interaction (HSI), Ultrasound.

I. INTRODUCTION

The communication among humans is based on a multi-modal system, which includes not only verbal communication but also face and body expressions to intensify the meaning of the verbal content. The Human System Interaction (HSI) trend is evolving, leading to the research of emerging technologies that mimic this natural communication, minimizing the use of interfaces like touchscreens, buttons or sliders. Well known virtual personal assistants such as Alexa or Siri, developed by Amazon and Apple respectively which allow communication with the system using only voice commands. There are also several systems that introduce gesture control to the system, i.e. SoundWave [1], AudioGest [2], Dolphin [3], or UltraGesture [4]. All of them use low frequency ultrasound signals to recognize between 5 and 12 gestures, which are mostly based on Doppler shift effect (frequency variation due to movement) while running the recognition algorithms on PC or Smartphones.

The aim of this work is to prove the possibility to develop a system able to detect gestures based only on ultrasonic signals and to execute the signal processing in Edge devices,

without using neither a PC nor a cloud environment. For testing, a set of 7 gestures plus idle has been defined, being possible to combine them to increase the recognized gestures. In order to recognize them, 2 transceivers will be used, since it is the minimum number of transceivers required to detect 2 dimensional gestures.

This device works as an active sonar system: it transmits ultrasonic waveforms, which are reflected back when they collide with any solid obstacle, to its environment. Then the transceivers receive these indirect echo signals in order to locate the echo produced by the obstacle. The transceivers are located on the same device. Thanks to this, it does not need an external synchronization signal to get the time-of-flight (ToF) value , which is the time between the transmitted signal emission and the echo signal reception. These measurements enable the system to have a great resolution in the depth dimension due to the direct relation between time-of-flight and the distance between the reflector object and the system. This is an advantage over 2D cameras or Electric Near Field sensors, which are more sensitive to noise and need to infer the distance from the strength of the received signals.

However, it has low positioning accuracy when it comes to the lateral range. In spite of higher processing time, it could be solved by adding more devices to the system, getting a combination of time-of-flights estimations between them.

This article is structured as follows: Section II introduces the state of the art in Ultrasound technologies for gesture recognition and the advantages of use Edge Computing for this purpose. Section III explains in detail the system developed in this work, as well as the firmware developed for the signal acquisition and ToF calculation. Section IV describes the gestures defined for the experiment and the algorithms studied for the recognition and classification. Section V summarizes the results obtained. Finally, Section VI focuses on conclusions of this work.

II. PRIOR WORK / STATE OF THE ART
A. ULTRASOUNDS
Originally, ultrasound technology started to be used to increase the perception under the sea for navigation purposes, known as sonar devices [5]. However, ultrasounds were soon applied to medicine [6] and quickly found in more application fields, such as non-destructive testing methods [7].

Nowadays, ultrasounds are used for object recognition [8], which aim to reduce the power consumption, computation, and cost of current optical sensors. In [9], DasIvan et al. created an ultrasonic-based hand-gesture recognition device using a single piezoelectric transducer and an 8-element microphone array. Despite the fact that the accuracy was lower than in devices using optical sensors, it increased the number of gestures supported by a factor of 200 within the same energy budget. The developed system uses the Sound-Source Localization (SSL) algorithm.

However, other approaches have tried different techniques with the same goal. UltraGesture [4] uses the Channel Impulse Response (CIR) for finger motion perception and recognition, getting a resolution of 7 mm in the measurements. Soundwave [1], AudioGest [2], and Dolphin [3] measure the frequency variation of the hand in the incoming signal due to the movement of the user, known as Doppler effect. All three works use commercial speakers and microphones embedded in existing systems.

The difference among the previously commented systems are the developed algorithms for the gesture recognition. SoundWave [1] implements a threshold-based dynamic peak tracking technique to capture the Doppler shifts recorded by a laptop. Similarly, AudioGest [2] adds some of the signal contexts to the estimation of the hand in-air time, average waving speed as well as hand moving range. Smart mobile devices have also been used for a closer interaction with the user, using the same Doppler shift technique as the previous papers [3]. A further comparison of these studies will be shown in Section V.

Apart from large-scale gestures as studied in our paper, ultrasound signals have also been used for multiple gesture types. An example of this is the classification of micro-gestures based on the micro-Doppler effect. Sang Y. et al.

[10] and Zeng Q. et al. [11] proposed two different models for this purpose. The data to classify in these papers are seven and five finger-based gestures respectively. Both models are based on Recurrent Neuronal Networks (RNN) and Convolutional Neuronal Networks (CNN) to study the temporal evolution of the micro-Doppler images, achieving an accuracy over 90% in both cases.

One of the reasons for the integration of ultrasound sensors when using these techniques rather than other technologies is its robust behaviour against the ambient light or visibility changes. At the same time, while cameras or microphones can easily differentiate not only the gestures or voice commands, but also who is doing it, they may incur privacy concerns. Ultrasounds only get relevant information of the movement and, consequently, capture fewer attributes from the users, which hardens user tracking and identification but improves the privacy of the user.

One of the goals of the proposed system in this paper is to integrate it into different multi-purpose large systems. Therefore, in order to reduce the complexity of the integration of the ultrasound module, an Edge approach has been researched. This implies that the whole data is preprocessed in the device at the network edge instead of depending on external devices or services such as Cloud Computing. At the same time, this approach would increase privacy since the raw data is not transmitted but only the final processed gesture classification is. The next subsection gives details about the advantages of this approach as well as a deeper description of Edge Computing.

B. EDGE COMPUTING
Edge Computing [12] is aimed at reducing Cloud workload to process device data. To do so, some preprocessing and/or computing tasks are executed at the network edge when possible. Thus, Edge Computing is suitable in scenarios where low latency is required for the user, or where the end device application has time critical constraints [13].

At the same time, this technique ensures integrity and confidentiality of the information [14]. As a result of not communicating the information with external devices, the energy consumption for the data transmission is reduced [15]. By preprocessing the data in the device, the confidential information which is not relevant for the final task can be masked/deleted before being shared with an external device. This process also can be used to standardize the format of the transmitted data in order to create a shared format that all the devices can understand even if initially the format of each device was different [16]. This is especially relevant when multiple devices are collaborating as it is in the Internet of Things environment.

III. HARDWARE DESCRIPTION AND SIGNAL ACQUISITION
The proposed system uses two modules, as shown in Figure 1. The first one is used to control two transducers to generate the outgoing signal and acquire the incoming echo. This

module also calculates the time elapsed between the emission and the reception of the signal for each transceiver. This time is known as Time of Flight (ToF). The first module also integrates the analog circuitry needed for the echo signals amplification. The second module receives the ToF values and, after filtering them, performs the recognition algorithm to determine the gesture realized by the user. If needed, this module can integrate an external Neuroshield board, to perform the recognition algorithm, and control an external device (such as a led strip) to display the detected gesture.
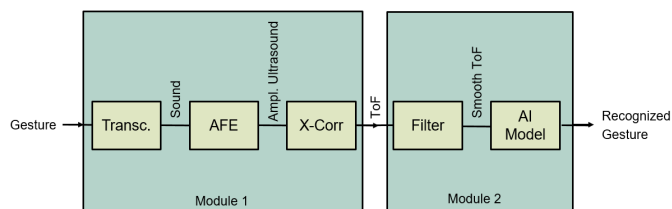

FIGURE 1: System diagram

Both modules are composed of a XMC4700 microcontroller performing the acquisition/recognition task, as well as a Bluetooth HC-05 device for the communication between them. This communication technology has been chosen to add a wireless channel between both modules to have flexibility on how to place them, but other technologies can be used as well.

The ultrasound transducers used in this work are based on a dual-backplate MEMS microphone technology allowing a combined use as an airborne ultrasonic transceiver and audio microphone. Those transducers need a low bias voltage and offer an audio performance of 68 dB(A) signal-to-noise ratio (SNR) and between 80 and 90 dB SNR in the ultrasonic frequency range. After the emission of the pulses, a free oscillation of the membrane (ringing) can override the incoming echo, producing a shadow zone that allows obstacle detection from 10 cm on [17].

A. SIGNAL EMISSION AND RECEPTION

The signal emission and reception are performed by the module 1, whose block diagram is shown in Figure 2. The signal to transmit is a square signal generated by a Pulse Width Modulation (PWM) block integrated into the processor. This signal is later transformed into an acoustic wave by one of the transducers. As soon as the PWM block finishes the pulse generation, the microcontroller starts collecting samples using two Analog Digital Converter (ADC) in parallel, one for each transceiver, to minimize time skew between samples. The echo received by the transducer, as an analog signal, carry some noise from the environment (as could be the use of buttons from a computer's keyboard or mouse, that have been seen to be harmful to the device's operating frequency). A band-pass amplifier was developed for this task, which amplifies the lower ultrasonic band (20 kHz to 100 kHz) while filters out all other frequencies. After this

filter, the signal must be digitalized by the microcontroller ADC module for further processing, as it is explained in the next subsection.
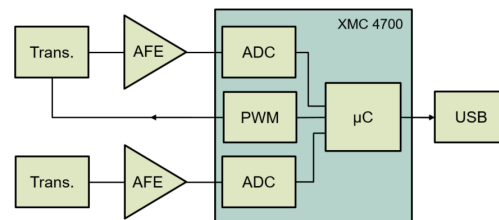

FIGURE 2: Transducer control and ToF calculation

B. TIME OF FLIGHT

After the signal is acquired it has to be processed to identify if there is an incoming echo, and the position of this if applicable. The ToF calculus has to be done while the following frame is being acquired, running both processes in parallel as shown in Figure 3.
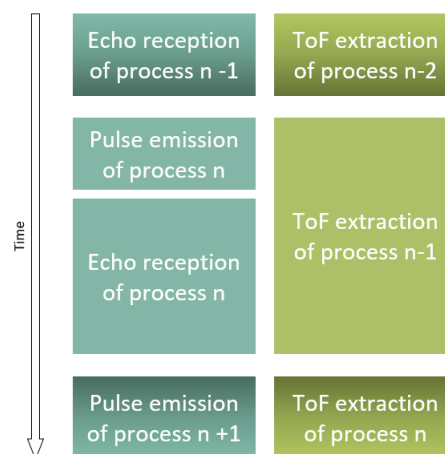

FIGURE 3: Firmware task parallelization to minimize execution time.

The signal can be processed in different domains to calculate the ToF, finding in the literature several methods for each domain, as collected by J. C. Jackson et al. [18]. and summarized in table 1.

Domain	Methods
Time	- Threshold Detection - Cross-Correlation
Fourier Phase-Based	- Single-Frequency Signals - Chirps and the Cross-Spectrum
Hybrid Models	- Biologically Inspired

TABLE 1: Example of ToF calculus techniques.

Some methods try to imitate the nature systems to calculate the ToF. for example, D. Hayward et al. [19] developed the

IEEE *Access*

"Biologically Inspired Ranging Algorithm (BIRA)" based on the bats hearing system for echolocation.

Other models are based in the frequency domain, as for example K.-N. Huang et al. [20] use the phased difference of a single frequency signal to calculate the ToF. Also, signal with more than one frequency component has been studied to calculate the desired parameter, as for example D. M. Cowell et al. [21] used chirp-signals to increase the accuracy of the estimated ToF. This approach also avoids multi-path problems and differentiates between several emitters.

Due to the low computation power required and good results, most works base this calculus on time domain methods, based i.e. on the amplitude of the incoming signal or in the cross-correlation of the echo with the sent (or expected) signal. The cross-correlation method reduces the high influence of noise in the amplitude method, since the cross-correlation, which acts as matched filtering, produces a time-domain signal with a maximum at the time when the echo was received [18] [22].

The ToF calculation proposed in this system can be divided in four steps as described in Figure 4. First, the acquired signal is cross-correlated with the template of the expecting echo, giving a maximum value where the expected and real echo overlap. Then, the envelope of the previous signal is obtained using a low pass filter. After that, the envelope is evaluated to extract the first cut with a dynamic threshold. This threshold represents the attenuation of the signal due to the distance traveled. It can be adjusted according to the ambient noise level of each specific scenario. Finally, the maximum of the cross-correlated signal is searched on a window with center in the threshold-envelope crossing value, giving the position of the ToF in number of samples. Once the number of ToF samples is determined, it can be easily converted to time knowing the ADC sampling frequency.

Using only one transceiver as emitter brings a non-desire effect in the ToF calculus. The distance from the obstacle to the transmitter is a direct relation with the ToF estimated, as shown in (1), but the ToF estimated in the signal of the second transceiver is a relation of the distance between the obstacle with both transceivers, as shown in (2). The solution to this effect will be further discussed in following sections.

$$ToF_1 = \frac{2d_1}{c_s} \qquad (1)$$

$$ToF_2 = \frac{d_1 + d_2}{c_s} \qquad (2)$$

Where ToF_n indicate the ToF for the transceiver n, d_n the distance between the target and the transceiver n and c_s the speed of the sound.

The proposed system is robust also to temperature changes. The speed of the sound in the air depends, among other environmental effects, on the air temperature [23]. This dependency is significant enough to allow the estimation of air temperature based on the difference between ToF measurement as shown by P.Annibale et al. [24]. Once more, the
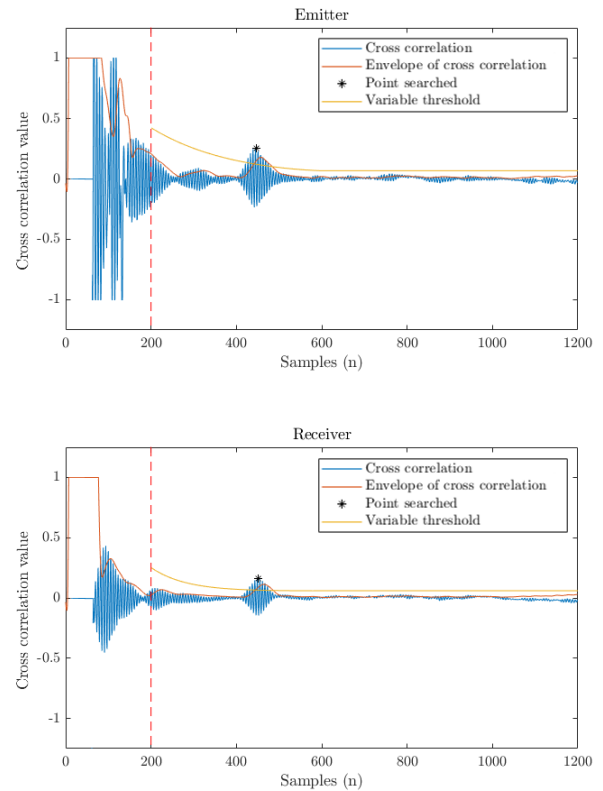

FIGURE 4: ToF calculus algorithm: cross-correlation signal (blue), cross-correlation signal envelope (red), threshold for echo detection (yellow) and peak value detected (black).

use of the relation between ToF of both transceivers provides the mitigation of this non desire effect.

IV. GESTURE RECOGNITION METHODS

Seven gestures, and idle, have been selected for this experiment: front push, front pull, right push, right pull, left push, left pull, static position, and no gesture. These gestures are well defined arm or hand movements in two dimensions to minimize the gesture complexity and reduce to two the required transceivers. Therefore, all gestures must be contained in this plane and so they are assumed to be in the front part of the sensors as shown in Figure 5. Otherwise, the system won't be able to track the gesture, due to the transceiver's unidirectional sensitivity and radiation pattern. This is an effect of the package to protect the membranes and electronics, which is also used to increase the strength of the emitted signal.

These gestures are measured using both transceivers simultaneously. By extracting the ToF from each sensor in each moment, as explained in IV-A by (1) and (2), it is possible to determine the movement direction and the region of the plane where the movement has been done.

Four individuals performed these gestures in different conditions within a distance of 15-50 cm from the device
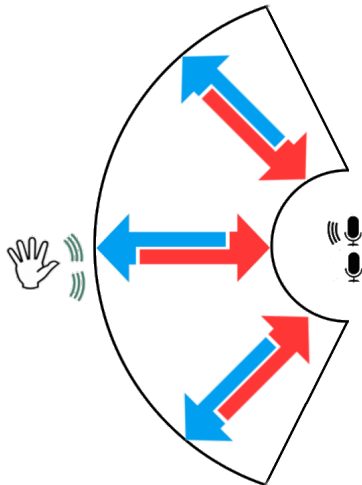
IEEE *Access*

FIGURE 5: Gestures diagram: push(red) and pull(blue) direction in the three different regions (Top view).

to collect data from different conditions. Each individual repeated each gesture 4 times per session during 20 sessions. These gestures have a variable length depending on the subject and the specific time, which helps to create a more diverse dataset. The average time length of these gestures was approximately 3 seconds after a review of average length on hand gestures. The frequency used for recording the ToF samples was 30 Hz. Nevertheless, the time length of the whole gesture is not a critical factor, since each gesture is classified multiple times during its performance. Therefore, even if a gesture is short, as far as it lasts for the required 7 ToF samples (250ms), it will be correctly classified. However, the speed of the gesture may affect on a larger scale since a lower hand speed will result in a smaller variation of the ToF. If this happens, the system may classify this gesture as idle due to its low variance of the position.

The final data-set created contains 3150 gesture samples where each gesture sample consists of a number ToF samples from each transceiver as shown in Figure 6. The specific number of ToF samples will be commented in Section IV-B. Out of all the gestures samples, 80% were used during the training process and the remaining 20% were used for testing the final system.
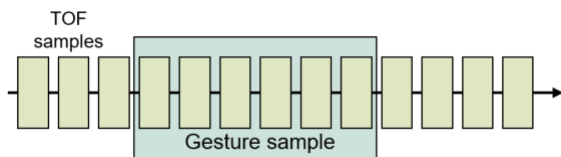

FIGURE 6: Gesture sample creation

A. FILTERING THE RAW TOF DATA

After preprocessing the raw ToF data extracted from the transceivers, the data needs to be filtered in order to remove

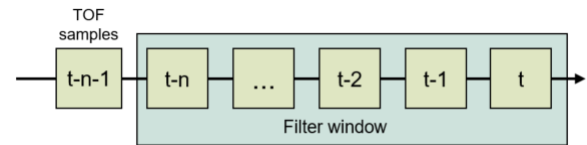outlier points as well as reconstruct the ToF signal when possible.

FIGURE 7: Filter window

While multiple filtering techniques may be applied in this scenario, the speed of the system when applying the filtering technique has to be taken as a constrain in order to avoid creating a bottleneck at this point. Therefore, a filtering technique where the ToF data is compared with the n previous ToF samples has been designed resulting in a smooth filter specific for this application. This filter has been designed to take into account the most frequent and relevant problems detected in the raw signal, such as missing information or measurements when the sensor is saturated. As a result of this, it is more suitable than a general purpose smooth filter.

The window approach used with the filtering technique described is shown in figure 7. The goal of this filter is to remove outlier points and recover lost ToF samples. The dimension of the window of data that will be used with this filter has been researched to determine the optimal size. The compared parameters for these filters are the execution time as well as the noise reduction. Table 2 shows all the compared dimensions.

Window size	Execution time (us)	Noise reduction
8	7.42	74.86 %
10	9.87	84.70 %
11	10.92	85.30 %
15	14.1	85.92 %
20	18.3	86.27 %

TABLE 2: Comparison of multiple sizes for the window of the filter technique.

The final size of the window is 11 ToF samples. This decision was based on the trade-off between the noise reduction and the execution time. Larger window filters lead to latency problems since its execution and the later classification would exceed the time limit of 33 us. At the same time, these filters only provide, as maximum, a 0.97% improvement respect the chosen filter regarding noise reduction. The effect of applying this filter in the ToF data can be observed in figure 8.

This preprocessing has proven to increase the accuracy of the gesture classification, as shown in Section V, where this fact will be further explained.

The filtered ToF samples of some of the studied gestures using the previous filtering technique are shown in figure 9 for a deeper understanding of the data used in this paper.

Besides the remaining noise in the signal after the filtering process, it is possible to obtain high classification accuracy
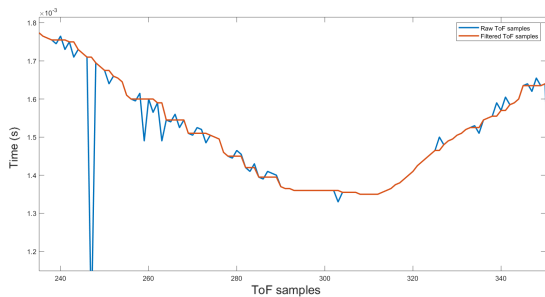
FIGURE 8: ToF data before and after applying filter.

(a) Left push **(b)** Left pull
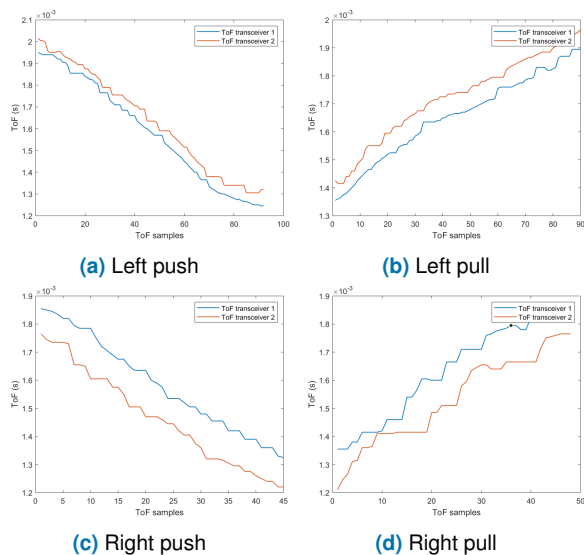
(c) Right push **(d)** Right pull

FIGURE 9: Filtered ToF samples of left and right push and pull gestures.

thanks to the researched algorithms. During the training process, at the same time the AI models learn to classify the input data, they learn as well to adapt themselves to the noise of the signals. Further explanations of these algorithms are done in Section IV-B.

B. ALGORITHMS

Multiple classification algorithms were applied to the gathered data aiming to compare the gesture recognition accuracy based on the collected data explained in the previous sections. The data used for the classification has been explained in Subsection IV, where Figure 6 shows how each gesture sample is created as a succession of ToF samples from both transceivers. This enables the system to learn the time evolution of the signal without using complex algorithms such as LSTM neural networks.

Each time a new ToF sample is received, the window slides creating a new gesture sample including the new ToF sample and removing the oldest one. The sliding window enables the system to generate more gesture samples for the learning phase than dividing the whole data-set into sub-datasets of n ToF samples.

Since the algorithms used for the classification are based on a supervised learning approach, the ToF data does not have to be preprocessed to obtain the real distances with respect to each transceiver. At the same time, the algorithms learn to overcome the possible remaining noise in the data after the first filter explained in Subsection IV-A.

Finally, from each gesture sample, the slope of the gesture sample from each transceiver as well as the difference between their mean values were used as input features for the classification algorithms.

The relevant information of the gesture data for its classification is the evolution of the value of the ToF signals. Therefore, a study to decide the number of ToF samples contained in each gesture sample was carried out. As the gesture data will be preprocessed to extract the previously explained features, the number of inputs for the algorithms is independent from the number of ToF samples per gesture sample. The comparison was based on the final accuracy achieved in Multilayer Perceptron (MLP) [25] that will be commented in this section, as shown in Table 3.

Number of ToF samples	Final accuracy
4	84.78 %
6	92.63 %
7	92.87 %
8	92.87 %
10	90.15 %
12	90.12 %

TABLE 3: Comparison of multiple number of ToF samples per gesture sample.

As a result of this study, the number of ToF samples per gesture sample was set to 7. The reason for this decision is its high accuracy in the MLP model as well as its reduced number of samples. The latest reason leads to an increase of the number of gestures samples created. This is beneficial during the training phase of the models. Its higher accuracy in comparison with the cases of a higher number of ToF samples is due to the fact this increase leads to problems during transitions between gestures.

Three algorithms have been researched in this paper:

- **Deep Learning model.** Different structures of Deep Neural Networks (DNN) were researched, such as MLP [25], Long Short Term memory (LST) DNN [26] and Convolutional Neural Network [27]. Since the features used for the classification do not require a time evolution study or a further feature extraction, we concluded the MLP was the structure that fits in this application among the DNN structure researched. This decision was based on the time required to re-train the DNN in case new gestures are added to the system as well as its speed to compute the result. In case any of the other DNN structure were implemented, the latency of the system would increase leading to bottleneck problems in the classification step of the pipeline.

IEEE *Access*

The proposed MLP model was designed keeping in mind the number of layers as well as artificial neurons while achieving high accuracy results. The chosen structure is an MLP of 4 layers as Figure 10 shows. The input layer includes 3 artificial neurons, which represent the number of features that will be fed into this DNN. Following the input layer, there are two hidden layers with 6 and 9 neurons respectively. The output layer contains 8 neurons to match the number of gestures (including idle) studied in this paper. In the structure, batch normalization layers have been added between each layer to increase the stability of the DNN.

As a result, this model could be implemented in an Edge Device for the inference process due to its low memory requirements as well as the speed to process the input data.
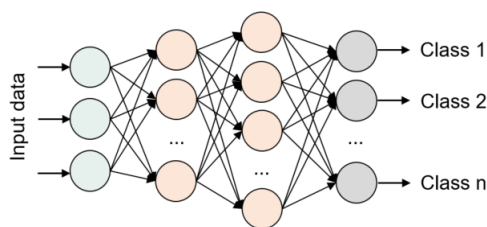

FIGURE 10: MLP network structure.

- **Deep Learning model based on Neuroshield device.** Another approach researched in this paper was the implementation of the classification task in the Neuroshield device [28]. This device includes 576 artificial neurons programmed with a radial basis activation function [29] rather than the previously commented DNN. This activation function computes the distance, in the feature representation plane, of the established center of each neuron with the input data as shown in Figure 11. After calculating all the distances, it calculates which neuron is the closest to the input data and, in case the distance is smaller than the activation distance, the input activates the corresponding artificial neuron.

  This optimized algorithm, apart from moving the inference stage to the network edge due to its reduced latency, enables the execution of the training of the AI model at the network edge. The limitations of this model fall on the fact the DNN designed for this device must be trained using the same technique, radial basis activation function.

- **Decision Tree model.** This model is based on a set of rules which are defined during the training stage in order to classify the gesture by comparing the input data with a list of conditional clauses where the data is divided into different decisions according to a certain parameter [30] leading to a final decision based on the results of these conditional clauses. This model is less computing-power demanding due to its simplicity to classify a new data sample. At the same time, this simplicity makes it
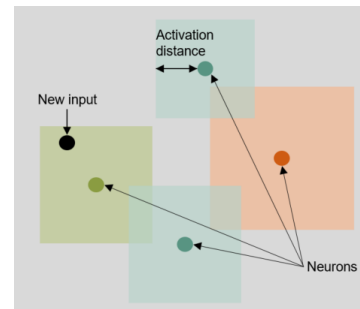

FIGURE 11: Neuroshield activation function structure.

difficult to maintain its accuracy when the complexity of the data increases.

The features fed into the classification techniques were the same: the slope of the ToF signal measured from the first transceiver and the average value of the last seven ToF samples as well as the difference of the mean values of the ToF signals measured with both transceivers. The same postprocessing technique has been applied to all the previous algorithms in order to further improve their accuracy while still being able to compare them. The postprocessing technique applied is a sliding window to extract the most frequent classification results in the last 5 classification results. Therefore, outlier classification results are filtered, maintaining a slow and continuous change between gestures. The improvement of the accuracy when applying this technique can be observed in Section V.

V. RESULTS

The results obtained with the previously explained techniques are presented in this section using the same data to ensure a correct comparison of the algorithms.

Due to the fact that all these techniques accomplish with the time restriction of the system, the compared parameter in this section is the accuracy, which is measured in this experiment as correct classifications over all the classifications.

The Table 4 shows the accuracy achieved using each classification approach. At the same time, this table compares the accuracy results obtained when using the raw signal (first column), the filtered ToF data (second column), and using all the previously explained preprocessing techniques as well as the window to filter the output classification results.

Classification technique	Acc. 1	Acc. 2	Acc. 3
MLP	84.18%	91.16%	92.87%
Neuroshield	95.69%	97.75%	98.4%
Decision Tree	91.8%	92.15%	96.94%

TABLE 4: Accuracy results without any filter or window (acc. 1), without the window (acc. 2) and using all the filtering techniques (acc. 3).

The results obtained with the Neuroshield device achieved the highest accuracy among the researched techniques, both scenarios of not applying or applying the postprocessing

technique. However, this system lacks the flexibility the other two techniques can provide due to the fact that this device can only execute one kind of DNN and it can not be transferred to another device different from a Neuroshield device.

The Decision Tree algorithm achieved a final accuracy of 5.6% and 1.46% lower than the Neuroshield device, without the postprocessing and including it respectively. Nevertheless, this technique is the less power requiring due to its simplicity in comparison with the DNN structures presented in the paper.

The MLP classificator achieved a final accuracy of 6.59% and 5.53% lower than the Neuroshield devices, without the postprocessing and including it respectively. In spite of achieving the lowest accuracy among these techniques, this one provides the highest flexibility since the structure of the DNN and the activation function can be modified easily as well as transferred to other devices.

FIGURE 12: MLP confusion matrix.

FIGURE 13: Neuroshield algorithm confusion matrix.

FIGURE 14: Decision tree confusion matrix.

For a deeper comparison of the accuracy achieved for each gesture, Figures 12, 13 and 14 show the confusion matrix of the final algorithms (including all the filtering techniques). It is possible to observe how all the researched algorithms achieve high accuracy for all the gestures, being the lowest one the accuracy achieved for the gesture 5 (left push), 83.1%, when using the MLP algorithm. Therefore, we can conclude all these models can generalize the data properly. As previously commented, these tables also show how the MLP model achieves the lowest accuracy results for all the gestures among the researched algorithms. The main difference we can observe from these confusion matrices is the error distribution. While the errors in the MLP and decision tree models are distributed across all the gestures, the errors of the Neuroshield model are concentrated in the last 4 gestures.

Another relevant factor to compare among the researched algorithms is the memory consumption of the different models since this is one of the restrictive parameters in Edge Devices. Table 5 shows this comparison, where it is possible to observe how the MLP model, even when its accuracy is approximately 5% lower than the best model of the Neuroshield device, leads to a memory consumption reduction for the model of an 83.1%.

Classification technique	Model size
MLP	23KB
Neuroshield	136KB
Decision Tree	273 KB

TABLE 5: Comparison of the size of the researched algorithms.

The latency of these models has not been compared since all of them satisfied the restriction of the 33ms established by the hardware providing a classification result for any new data before receiving the next one.

A comparison of the studies described in Section II is

Studies	No. of Gestures	Accuracy	Method	Hardware
SoundWave	5	86.7 – 100%	Doppler shift	1 microphone 1 speaker
AudioGest	6	95.1%	Doppler shift	1 microphone 1 speaker
Dolphin	24	93%	Doppler shift	1 microphone 1 speaker Gravity sensor
UltraGesture	12	91.42 – 98.58%	Channel Impulse Response (CIR)	4 microphones 1 speaker
Microsoft	5	64.5 – 96.9%	CNN-LSTM	8 microphones 1 transceiver
Proposed system	8	84.18 – 98.4%	AI models	2 transceiver

TABLE 6: Comparison of state-of-the-art techniques for gesture recognition with ultrasounds.

presented in Table 6. Even though it is not possible to compare the performance of the algorithms due to the lack of a common public dataset as well as the difference in the data structure each technique requires, significant parameters of each system can be compared. The future development of gesture recognition systems based on ultrasound technology could benefit from a common data framework, thus allowing the cooperative development of algorithms with much more data and from different sources and conditions.

One of the features that we can compare is the devices integrated into these systems. It is possible to observe how the majority of the researchers are basing the systems on a multi-sensor approach where a separated microphone and speaker are integrated. On the other hand, our proposed system tries to reduce the number of devices integrating transceivers.

VI. CONCLUSION

The system presented in this paper has been proven to be able to measure ToF signals that can be later used to recognize multiple gestures by the integration of two transceivers. Due to the optimization of the preprocessing correlation technique to extract the ToF from the echo signals and the specific design of the firmware to enable the parallelization of concurrent processes, the system can be implemented as an Edge Device. This system does not require any external device or cloud server to preprocess the information.

At the same time, by using the Neuroshield device, which enables the implementation of an AI classificator at the network edge, or the MLP implemented in an Edge Device, it is also possible to execute the full process from data gathering to extract the classification at the network edge while maintaining high accuracy results. It has been shown how the researched algorithms provided high accuracy, where the best result is extracted from the Neuroshield with a 98.4% accuracy.

The memory sizes of the models are also a relevant feature to compare since it is one of the main constrains in Edge Devices. Because of this, this feature has been taken into account during the optimization of the models. As a result

of this, the size of all the proposed models has been reduced, i.e. the proposed MLP, whose size is 23 KB while it stills achieves an accuracy of 92.87% in our dataset.

REFERENCES

[1] Sidhant Gupta, Daniel Morris, Shwetak Patel, and Desney Tan. Sound-wave: using the doppler effect to sense gestures. Proceedings of the SIGCHI Conference on Human Factors in Computing Systems, pages 1911–1914, 2012.

[2] Wenjie Ruan, Quan Z Sheng, Lei Yang, Tao Gu, Peipei Xu, and Longfei Shangguan. Audiogest: enabling fine-grained hand gesture detection by decoding echo signal. Proceedings of the 2016 ACM international joint conference on pervasive and ubiquitous computing, pages 474–485, 2016.

[3] Yang Qifan, Tang Hao, Zhao Xuebing, Li Yin, and Zhang Sanfeng. Dolphin: Ultrasonic-based gesture recognition on smartphone platform. 2014 IEEE 17th International Conference on Computational Science and Engineering, pages 1461–1468, 2014.

[4] Kang Ling, Haipeng Dai, Yuntang Liu, and Alex X Liu. Ultragesture: Fine-grained gesture sensing and recognition. 2018 15th Annual IEEE International Conference on Sensing, Communication, and Networking (SECON), pages 1–9, 2018.

[5] Jacques Lewiner. Paul langevin and the birth of ultrasonics. Japanese Journal of Applied Physics, 30(S1):5, jan 1991.

[6] Aladin Carovac, Fahrudin Smajlovic, and Dzelaludin Junuzovic. Application of ultrasound in medicine. Acta Informatica Medica, 19(3):168, 2011.

[7] M G Silk. Ultrasonic transducers for nondestructive testing.

[8] Y. Gao, M. A. Maraci, and J. A. Noble. Describing ultrasound video content using deep convolutional neural networks. 2016 IEEE 13th International Symposium on Biomedical Imaging (ISBI), pages 787–790, 2016.

[9] Amit Das, Ivan Tashev, and Shoaib Mohammed. Ultrasound based gesture recognition. 2017 IEEE International Conference on Acoustics, Speech and Signal Processing (ICASSP), pages 406–410, 2017.

[10] Yu Sang, Laixi Shi, and Yimin Liu. Micro hand gesture recognition system using ultrasonic active sensing. IEEE Access, 6:49339–49347, 2018.

[11] Qinglin Zeng, Zheng Kuang, Shuaibing Wu, and Jun Yang. A method of ultrasonic finger gesture recognition based on the micro-doppler effect. Applied Sciences, 9(11):2314, 2019.

[12] Dinesh Dash Partha Pratim Ray and Debashis. Edge computing for Internet of Things: A survey, e-healthcare case study and future direction. Network and Computer Applications, 140:1–22, 2019.

[13] M. Satyanarayanan. The emergence of edge computing. Computer, 50(1):30–39, 2017.

[14] Sara Casado-Vara Roberto Sittón-Candanedo Inés Alonso Ricardo Corchado Rodríguez, Juan Rodríguez. A Review of Edge Computing Reference Architectures and a new Global Edge Proposal. Future Generation Computer Systems, 2019.

[15] J. Cao Q. Zhang Y. Li W. Shi and L. Xu. Edge Computing: Vision and Challenges. IEEE Internet of Things Journal, 3(5):637–646, 2016.

IEEE *Access*

[16] W. Yu et al. A Survey on the Edge Computing for the Internet of Things. IEEE Access, 6:6900–6919, 2018.

[17] Sebastian Anzinger, Christian Bretthauer, Johannes Manz, Ulrich Krumbein, and Alfons Dehé. Broadband acoustical mems transceivers for simultaneous range finding and microphone applications. 2019 20th International Conference on Solid-State Sensors, Actuators and Microsystems & Eurosensors XXXIII (TRANSDUCERS & EUROSENSORS XXXIII), pages 865–868, 2019.

[18] J. C. Jackson, R. Summan, G. I. Dobie, S. M. Whiteley, S. G. Pierce, and G. Hayward. Time-of-flight measurement techniques for airborne ultrasonic ranging. IEEE Transactions on Ultrasonics, Ferroelectrics, and Frequency Control, 60(2):343–355, 2013.

[19] G Hayward, F Devaud, and JJ Soraghan. P1g-3 evaluation of a bio-inspired range finding algorithm (bira). 2006 IEEE Ultrasonics Symposium, pages 1381–1384, 2006.

[20] Ke-Nung Huang and Yu-Pei Huang. Multiple-frequency ultrasonic distance measurement using direct digital frequency synthesizers. Sensors and Actuators A: Physical, 149(1):42–50, 2009.

[21] David MJ Cowell and Steven Freear. Separation of overlapping linear frequency modulated (lfm) signals using the fractional fourier transform. IEEE transactions on ultrasonics, ferroelectrics, and frequency control, 57(10):2324–2333, 2010.

[22] Jian Chen, Fan Yu, Jianxin Yu, and Lin Lin. A three-dimensional pen-like ultrasonic positioning system based on quasi-spherical pvdf ultrasonic transmitter. IEEE Sensors Journal, 2020.

[23] Dennis A Bohn. Environmental effects on the speed of sound. Audio Engineering Society Convention 83, 1987.

[24] Paolo Annibale, Jason Filos, Patrick A Naylor, and Rudolf Rabenstein. Tdoa-based speed of sound estimation for air temperature and room geometry inference. IEEE transactions on audio, speech, and language processing, 21(2):234–246, 2012.

[25] Marius-Constantin Popescu, Valentina E. Balas, Liliana Perescu-Popescu, and Nikos Mastorakis. Multilayer Perceptron: Architecture Optimization and Training with Mixed Activation Functions. BDCA'17. Association for Computing Machinery, New York, NY, USA, 2017.

[26] Sepp Hochreiter and Jürgen Schmidhuber. Long short-term memory. Neural computation, 9:1735–1780, 1997.

[27] T. A. Mohammed S. Albawi and S. Al-Zawi. Understanding of a convolutional neural network. International Conference on Engineering and Technology (ICET), Antalya, 2017, pages 1–6, 2017.

[28] General Vision. Neuroshield.

[29] S. Elanayar V.T. and Y. C. Shin. Radial basis function neural network for approximation and estimation of nonlinear stochastic dynamic systems. IEEE Transactions on Neural Networks, 5(4):594–603, 1994.

[30] S. R. Safavian and D. Landgrebe. A survey of decision tree classifier methodology. IEEE Transactions on Systems, Man, and Cybernetics, 21(3):660–674, 1991.

JAVIER MENDEZ received the B.Sc. degree in electronics engineering from the University of Granada in 2018. Then, in 2019 he got the M.Sc. degree in electronics, robotics and automatics engineering from the University of Sevilla, Spain, where he got the award as the head of the he graduating class. Since October 2019 he joined Infineon as a PhD candidate in collaboration with the University of Granada and worked on artificial intelligence at the network edge as well as sensor fusion algorithms. His current research interests include edge computing, deep learning and sensor fusion.

MIGUEL MOLINA received the B.Sc. degree in electronics engineering from the University of Granada in 2019. Then, in 2020 he got the M.Sc. degree in Electronic Systems Engineering from the Polytechnic University of Madrid. He joined Infineon Technologies AG in August 2020 as a PhD candidate, also in collaboration with the University of Granada. He is currently working on applications of Sensor Fusion for drones and into hardware implementations of Neural Networks, especially for Spiking Neural Networks (SNN). His main research interests are FPGAs, edge computing, Neural Networks and Industry 4.0.

ENCARNACIÓN CASTILLO received the M.Sc. and Ph.D. degrees in electronic engineering from the University of Granada, Granada, Spain, in 2002 and 2008, respectively. From 2003 to 2005, she was a Research Fellow with the Department of Electronics and Computer Technology, University of Granada, where she is currently an Associate Professor. During her research fellowship, she carried out part of her research with the Department of Electrical and Computer Engineering, Florida State University, Tallahassee, FL, USA. She has authored over 50 technical papers in international journals and conferences. Her current research interests include the protection of IP protection of very large-scale integration (VLSI) and field-programmable gate arrays-based systems, as well as residue number system arithmetic, VLSI and FPL signal processing systems, and the combination of digital and analog programmable technologies for smart instrumentation for biosignal processing. She also serves regularly as a reviewer for IEEE journals.

BORJA SAEZ received the B.Sc. degree in Telecommunication Engineering from the University of Granada in 2015. Then, in 2017 he got the M.Sc. degree in Telecommunication Engineering from ICAI, Universidad Pontificia Comillas de Madrid, Spain. He joined Infineon Technologies AG in September 2017 as a PhD candidate, also in collaboration with the University of Granada. He is currently working on applications of signal processing and gesture recognition. His current research interests include Artificial Intelligence, Deep Learning and Human system integration.

MANUEL PEGALAJAR graduated in Computer Engineering in 2003. He finished the Ph.D. degree on time series prediction, parameter identification, and neural networks in 2006.,He is currently a full-time Teacher with the Department of Computer Science and Artificial Intelligence, University of Granada, Granada, Spain. His main interests are neural and social networks, evolutionary optimization, and fuzzy systems. He has also worked in multivariate image analysis and real-time control tasks.

IEEE *Access*

DIEGO P. MORALES received the B.Sc., M.Eng., and Ph.D. degrees in electronics engineering from the University of Granada, in 2001 and 2011, respectively.,Since 2001, he has been an Associate Professor with the Department of Computer Architecture and Electronics, University of Almeria, before joining the Department of Electronics and Computer Technology, University of Granada, in 2006, where he currently serves as a Tenured Professor. He is the Co-Founder of the Biochemistry and Electronics as Sensing Technologies (BEST) Research Group, University of Granada. His current research interests include low-power energy conversion, energy harvesting for wearable sensing systems, and new materials for electronics and sensors. He has coauthored more than 80 scientific contributions.

• • •